**Article:**
Whiteley, J., Liew, A., He, L. et al. (2023) Engineering design of optimized reinforced concrete floor grillages. Structures, 51. pp. 1292-1304. ISSN: 2352-0124

https://doi.org/10.1016/j.istruc.2023.03.116

Structures 51 (2023) 1292–1304

Contents lists available at ScienceDirect

Structures

journal homepage: www.elsevier.com/locate/structures

# Engineering design of optimized reinforced concrete floor grillages

J. Whiteley, A. Liew *, L. He, M. Gilbert

*Department of Civil and Structural Engineering, The University of Sheffield, UK*

ARTICLE INFO

*Keywords:*
Grillage
Optimization
Reinforced concrete
Slab
Sustainability
Floorplate

ABSTRACT

A new reinforced concrete beam grillage floor system is proposed as a lightweight alternative to traditional solid flat or waffle slabs used in construction. For the first time, beam grillage optimization has been paired with design code compliant floor plate design, for single and multi-bays of a building. The investigated floor slabs are novel, in that the depths of the grillage T-beams and their reinforcement are tailored for the local strength demands. This engineering efficiency gives rise to significant savings of approximately 40–50% in the quantities of concrete and steel needed compared to flat slabs. For the multi-bay studies, it was found that moving the location of the supporting columns could further decrease the volume of material required, by over 50% compared to a standard grid layout. Given the urgent need to reduce the volume of material consumed in construction projects, this appears to challenge traditional floorplate layouts. The research shows that digital optimization tools can be paired with standard design code rules to deliver significantly more sustainable building designs, though these benefits need to be balanced against the construction challenges associated with the more complex geometries that generally result.

## 1. Introduction

Concrete floor systems have been used for structural engineering applications since the latter half of the 19th century. They are relatively quick and inexpensive to construct and are also long lasting and robust, with good fire performance. This has led to them being widely used across the world [1]. However, particularly in recent years, concerns have been raised about the environmental impact of concrete construction in general, of which the contribution of concrete floor slabs is significant. There is thus an imperative to develop more environmentally friendly alternatives to traditional systems.

Flat slabs constructed using reinforced concrete (RC) are quick to construct and offer a flexible floor plan [2], ensuring their popularity throughout the 20th and early 21st centuries. In contrast, RC waffle slabs became popular in the 1960's and 1970's [3], but are less commonly used today. Compared with waffle slabs, flat slabs provide a lower overall building height and are simpler to design. However in flat slabs, often substantial regions of concrete are assumed cracked in design, such that the structural contribution of these regions is low in comparison to the dead weight [4]. Waffle slabs remove some of this under-utilized material, and as a result, are usually stiffer, lighter, span further, and are less susceptible to vibration serviceability issues than flat slabs. But their construction is more labour intensive and, as well as resulting in deeper floor depths, cladding costs are likely to be increased [2]. Fig. 1 shows four conventional reinforced concrete slab types, showing the use of either flat slabs or slabs with downstand elements.

More recently a wide range of innovative floor systems have been developed to improve the structural efficiency of RC slabs. These include slabs containing voids made from plastic (typically high-density polyethylene) void formers or air filled plastic spheres (e.g. BubbleDeck or Cobiax) [5]. These systems remove under-utilized material around the centre of the floor cross-section, though need to be used with care as there have been instances of shear failures [6]. Precast hollowcore slabs are also common, manufactured using an extrusion process that leaves an internal void. Alternatively, insulation material can be used in place of a void, such as in the Super Light Deck (SL-Deck) system developed at the Technical University of Denmark [7].

Slabs incorporating ribs can also be employed, for example, the Italian architect and engineer Pier Luigi Nervi famously patented a novel form of RC waffle slab (Fig. 2) in 1949, using a complex pattern of curving downstand ribs aligned to the lines of principal bending moment [8]. More recently, waffle slabs using downstand ribs incorporating integrated service voids have been developed, such as that seen in Fig. 3, which shows the efficient Holedeck floor system.

The need to limit greenhouse gas emissions to avoid the most catastrophic effects of climate change [10] is providing fresh impetus to develop more efficient floor systems. It is estimated that the building and construction sector accounts for around 40% of energy and process related emissions in developed countries, exceeding even

* Corresponding author.
*E-mail address:* a.liew@sheffield.ac.uk (A. Liew).

https://doi.org/10.1016/j.istruc.2023.03.116
Received 20 October 2022; Received in revised form 22 February 2023; Accepted 21 March 2023
Available online 28 March 2023

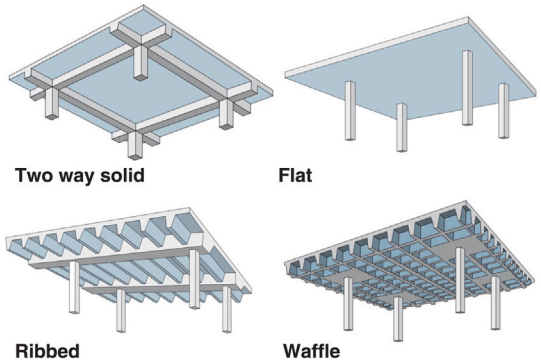


**Fig. 1.** Conventional reinforced concrete floor types used in construction, comprising flat slab regions with or without downstand elements (image: MPA The Concrete Centre).

**Fig. 2.** Gatti Wool Factory (Rome, 1951) by Pier Luigi Nervi, showing curved downstand beams on a regular column grid [9].

**Fig. 3.** Holedeck reinforced concrete floor system H0-45, with perforated beams to facilitate MEP services integration (image: HOLEDECK).

contributions from the industrial and transportation sectors [11,12]. Embodied carbon has been taking a growing share of total building related emissions, in comparison to operational emissions (related to a building's use) [13] that have been declining. This is because the embodied energy associated with commonly used structural materials is known to be difficult to decarbonize [14], whereas large efficiency gains in building services have been seen in recent years [13]. The environmental impact of traditional concrete construction is well documented; historically, almost a tonne of $CO_2$ has been emitted for each tonne of concrete produced. Since manufacturing processes have improved over the past few decades, it has been suggested that further improvements may be hard to secure [14,15]. Several billion tonnes of cement are produced annually [16,17] to service the concrete industry, with Ordinary Portland Cement (OPC) being the most common cement type used. Recent estimates have suggested cement could account for up to 8% of total anthropogenic global $CO_2$ emissions [16,18]. Cement also requires large amounts of energy to produce and concrete is highly water intensive and cannot easily be recycled upon demolition [19,20]. Despite these environmental concerns, the demand for concrete has been predicted to quadruple in the period between 1990 and 2050 [21], largely driven by increasing urbanization rates. It has also been suggested that increased material efficiency could offset this expected growth in demand [20].

Currently most of the material in a standard RC framed building is contained within the floor and roof slabs [22,23], which has led to significant research efforts being focused on the development of more economical and efficient RC floor systems. Shallow arching floors have been explored as an alternative to prismatic RC slabs, reducing the dead weight of a floor by 50–70% [4,24]. Textile reinforcement, such as carbon fibre reinforced polymer, has also been tested in RC slabs recently [4,25,26], reducing structural weight via a reduced requirement for concrete cover. Non-conventional materials such as recycled steel fibres and bamboo have also been evaluated as reinforcing materials in academic studies [27,28]. It has also been observed that T-beam and ribbed slabs, formed using a fabric formwork system [29], combined with efficient design practice, can reduce the dead load significantly [30]. Topologically optimized concrete beams have also been researched, cast using Computer Numerical Control (CNC) cut Styrofoam formwork [31], and similar methods have also been employed to identify efficient non-standard arrangements of internal reinforcement [32].

Fabricating the formwork for geometrically complex RC structures is challenging. Formwork fabrication using CNC cut wood, polyurethane or polystyrene has in recent years been used in industry for projects where complex geometries are involved, for example in 2013 in the Spencer Dock Bridge in Dublin [33], but this is known to be a comparatively energy intensive and wasteful method [34]. Hot wire foam cutting, flexible mould systems and the use of additive manufacturing have all been proposed as alternatives [35,36]. The use of 3D printed sand has facilitated the fabrication of formwork for ribbed slabs, as shown in Fig. 4 [37], and industrial 3D printed silica sand itself has been used to form shallow arching floors, which are efficient because compressive rather than flexural stresses are mobilized [38]. Layered concrete printing is also being explored for lightweight concrete ceilings [39]. For more typical waffle slabs, formwork usually comprises void formers (polystyrene or GRP) fixed to the top of table forms, onto which concrete is then poured [3], with lightweight blocks sometimes used as permanent formwork to create a flat soffit, albeit at the expense of some additional weight [7]. Digital engineering methods have also been applied in recent years, leading to new formwork systems and the development of 3D printing methods for concrete elements [40,41]. However, 3D printer bed capacities, the efficient incorporation of tensile reinforcement and the sustainability and mechanical properties of printable pastes are currently limiting factors [41,42].

In this paper a new RC floor system is proposed that takes advantage of a recently developed systematic numerical layout optimization method for grillages [43]. This is used to automatically generate

[H] 

**Fig. 4.** The Smart Slab: developed by the Digital Building Technologies Group, ETH Zurich. Based on a chosen layout of ribs, the final positions of ribs is optimized considering primarily geometric rather than stress or deformation considerations [37].

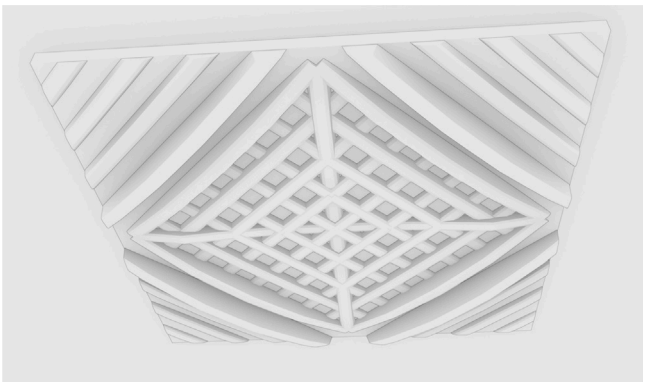

**Fig. 5.** Underside of a RC grillage optimized to transmit a uniformly distributed load to simple supports at the edges. The structure comprises a thin flat slab strengthened via variable depth downstands that form T-beams to carry sagging moments.

structurally efficient ribbed slab configurations, with the layout and dimensions of downstand ribs dependant upon the applied loading and support conditions. The numerical method used has similarities with previously developed truss optimization methods [44,45] and also builds on previous analytical grillage optimization studies carried out by Rozvany and co-workers [46]. Whereas in the latter work optimally reinforced concrete flat slabs were considered, with a number of slabs being tested to collapse to verify performance [47], here the focus is on generating efficient ribbed slab configurations. For other examples of layout/topology optimization being applied to reinforced concrete structures, readers are referred to the literature review recently undertaken by [48].

To illustrate the potential of the method developed, a sample optimized floor slab is shown in Fig. 5, depicting the underside of a simply-supported square slab. The downstand ribs which have constant width and trapezoidal section of varying depth, clearly differ from the downstands of a standard waffle slab, which are usually orthogonally arranged and of constant depth. The optimized slab comprises an arrangement of what are effectively T-beam ribs and makes more efficient use of both concrete and reinforcement. In this paper, details of the grillage optimization algorithm that identifies such arrangements is presented, together with details of how the output can be transformed into design code compliant engineering designs. The proposed workflow relies on digital engineering tools, both in the design stage and in the subsequent fabrication stage, when additional geometric complexity is introduced. While the construction industry has historically lagged behind the aerospace, automotive and consumer industries in terms of adoption of digital design and fabrication technologies [49], a consequence of this is that opportunities for development are substantial.

The lateral stability of a building has not been investigated in this research, as all applied loading, structural design and optimization has been in the vertical (gravity) direction. The important topic of lateral stability would involve the consideration of different lateral stability systems (cores, shear walls, frame action) and their interaction with the grillage floor system. It is commonly assumed in multi-storey building design that reinforced concrete floors act as diaphragms to transfer loads to the lateral resisting system; to this end, the grillage floor will still serve this purpose via the continuous top flange slab of the beam T-sections. Additional lateral stiffness, independent of dedicated shear walls and cores, will come from the connectivity of the ribbed floorplate structure with the supporting columns, creating additional lateral stiffness via frame action. The reader is referred to [50] for a study on the diaphragm condition for buildings with ribbed RC slabs, precast beam and block, steel decks and RC waffle flat slabs, where the degree of diaphragm flexibility was investigated for the different floor systems for moment resisting frames in the absence of shear walls and cores.

The paper is organized as follows. Section 2 provides an overview of the grillage optimization technique used and its application to the proposed grillage slab design. Section 3 describes the post-processing of the grillage optimization output to design Eurocode compliant grillage beam members. Section 4 outlines the structural engineering design of several one-bay floor systems as part of a comparative study, to assess the performance of the grillage system against traditional flat slab and waffle slab designs. Section 5 considers the effects of changing the locations of supporting columns on the output from the grillage optimization. Column layouts in representative larger floorplates are then explored. In Section 6 various practical design and fabrication issues are discussed, including how the design process could look like in practice, architectural considerations and opportunities that arise from use of the proposed floor system. Finally, conclusions are drawn at the end of the paper in Section 7.

## 2. Grillage optimization

The proposed optimized floor system is designed using the numerical grillage layout optimization approach first described in [43], where a beam grillage is a planar network of beams. This approach uses a 'ground structure', in this case consisting of a design domain discretized using $n$ nodes connected via $b$ tapered beams, with the cross-sectional area of each beam $i$ varying linearly from $a_{i1}$ to $a_{i2}$. The total volume $V$ of the structure can be written as:

$$V = \mathbf{l}^{\mathrm{T}}\mathbf{a}, \tag{1}$$

where $\mathbf{l} = \left[\frac{l_1}{2}, \frac{l_1}{2}, \frac{l_2}{2}, \frac{l_2}{2}, \ldots, \frac{l_b}{2}, \frac{l_b}{2}\right]^{\mathrm{T}}$ and $\mathbf{a} = \left[a_{11}, a_{12}, a_{21}, a_{22}, \ldots, a_{b1}, a_{b2}\right]^{\mathrm{T}}$ are, respectively, vectors of beam lengths and areas. At each node, moment equilibrium needs to be enforced in the $x$ and $y$ directions, and force equilibrium enforced in the $z$ direction. Denoting $m_{i1}$ and $m_{i2}$ as the moments at the two ends of beam $i$, the local equilibrium matrix can be expressed as:

$$\mathbf{B} = \begin{bmatrix} -\sin\theta_i & 0 \\ \cos\theta_i & 0 \\ \frac{1}{l_i} & -\frac{1}{l_i} \\ 0 & -\sin\theta_i \\ 0 & \cos\theta_i \\ -\frac{1}{l_i} & \frac{1}{l_i} \end{bmatrix}, \tag{2}$$

where $\theta_i$ is the angle of beam $i$ to the $x$ axis, and $l_i$ is its length. Also, if at this point it is assumed that the beam cross-sections are of uniform

depth, then $m_p^+$ and $m_p^-$ can be used to denote the limiting moments per unit area, and the yield condition of beam $i$ can be written as:

$$-m_p^- a_i \le m_{i1}, \qquad m_{i2} \le m_p^+ a_i. \tag{3}$$

The grillage layout optimization problem can then be written as:

$$\min_{\mathbf{a},\mathbf{q}} \quad V = \mathbf{l}^{\mathrm{T}}\mathbf{a} \tag{4a}$$

$$\text{s.t.} \quad \mathbf{B}\mathbf{q} = \mathbf{f} \tag{4b}$$

$$-\mathbf{m}_p^-\mathbf{a} \le \mathbf{q} \le \mathbf{m}_p^+\mathbf{a} \tag{4c}$$

$$\mathbf{a} \ge 0, \tag{4d}$$

where $\mathbf{q} = [m_{11}, m_{12}, m_{21}, m_{22}, \dots, m_{b1}, m_{b2}]^{\mathrm{T}}$ is a vector containing the moments at the two ends of each beam and $\mathbf{m}_p^+$, $\mathbf{m}_p^-$ are diagonal matrices containing respectively the sagging and hogging moment capacities, $m_p^+$ and $m_p^-$, of each beam. $\mathbf{B}$ is a global equilibrium matrix, assembled from the local matrices $\mathbf{B}_i$ and $\mathbf{f} = [m_1^x, m_1^y, f_1^z, m_2^x, m_2^y, f_2^z, \dots, m_n^x, m_n^y, f_n^z]^{\mathrm{T}}$ is the out-of-plane external loading applied at each node. This set of equations define a linear programming problem that can be solved efficiently using modern algorithms. The problem variables are the internal bending moments and cross-sectional areas at the ends of each beam.

The grillage optimization process usually starts with a design domain that is discretized with evenly spaced nodes interconnected by beam elements, shown with adjacent connectivity and for full connectivity in Fig. 6(a) and (b) respectively; the use of a full connectivity network ensures the grillage with the lowest volume is identified, albeit at the expense of additional computational effort and solution complexity. In this formulation out-of-plane (vertical) loading is applied as point loads to the nodes and boundary conditions are set as appropriate to enforce vertical restraint and/or moment fixity

The goal of the optimization is then to minimize the total structural volume (sum of all beam lengths multiplied by their cross-sectional areas); see solutions shown in Fig. 6(c) and (d). The linear programming formulation guarantees that these are globally optimal for the numerical discretizations employed, assuming the cross-section has fixed depth. However, in the case of the problem at hand, each beam in the grillage will be a RC T-beam forming the floor slab, and in a later post-processing step, the depths of the beams can be varied to give a near-optimal solution involving T-beams of varying depth that can withstand the required internal bending moments.

The output shown in Fig. 6 of the grillage layout optimization algorithm is a plan view of the beam section areas or bending moments across the grillage. It can be observed that the fully connected grillage can lead to many additional "thin" members that are of no practical use, and so, given that the structural volumes are often quite comparable, the faster running and cleaner adjacent connectivity grid is used in the present study. The bending moment distribution for the grillage can then be fed into the next stage of engineering design (see Section 3). Some practical parameters can already be imposed for the engineering design, such as differing values of hogging and sagging bending capacity for bending, and minimum or maximum areas/moments for all beams in the grillage, or for each beam individually. Note that many of the beam elements in the optimal solution will be found to have zero area.

Some other points to note that are of practical relevance are as follows: (1) optimizing for multiple load cases is possible in the grillage formulation, but is beyond the scope of the present study, (2) for the presented case studies later, uniformly distributed self-weight and super-imposed dead loads have been taken as discretized equivalent vertical nodal loads, and (3) the grillage optimization is based on ultimate limit state (plastic) design, which is discussed further in Section 3. For all of the grillage floor plate studies, the rib or downstand spacing was chosen as 1.0 m to represent a reasonable and clear separation between beam lines, but this can be freely chosen by the designer via the design domain discretization into nodes.

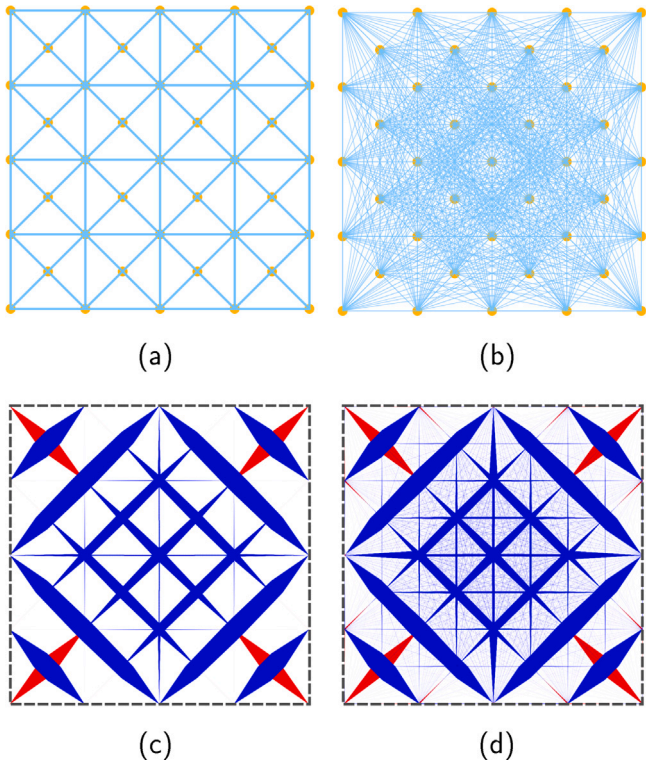


**Fig. 6.** Square grillage design problem: (a) nodes (orange dots) and nearest neighbour beam connections (light blue lines); (b) nodes and full nodal connectivity; (c) and (d) optimal grillage solution assuming uniform load, simple-supports and nodal connectivity. Blue and red lines correspond respectively to sagging and hogging beams, with line-width scaled to the magnitude of the bending moments.

## 3. Engineering design

This section describes how the output of the grillage optimization outlined in the preceding section can be used to engineer a new floor slab system. All engineering design calculations are carried out in accordance with Eurocode 2 (BS EN 1992-1-1:2004) [51], in conjunction with the UK National Annex [52].

As already noted, the optimal grillage solution comprises a network of tapered beams of the required moment capacity. This means that T-section beams, designed using standard methods, can be used to form a ribbed slab. For the sake of simplicity (in design and fabrication), here downstand rib widths are taken to be fixed, with the necessary moment capacity of each beam achieved by varying the section depth and/or the area of steel reinforcement. Due to the bespoke nature of the grillage layout in contrast to the fixed geometry associated with a traditional waffle slab, there will be many different cross-sections to design for across the floor slab. However, standard design tools available to the practising engineer, such as code compliant spreadsheets and software packages can be used to prepare the designs. Note that design shear forces are easily calculated by taking the derivative (slope) of the bending moment diagrams along each beam; a short programming script was written to facilitate this.

A cross-section of a representative T-section beam is shown in Fig. 7. Its moment resistance arises from the effective width $b_{\mathrm{eff}}$ of the concrete slab (or the section inverted with downstand width $b$ if hogging), with rectangular compressive stress block of depth $0.8x$, design stress $f_{\mathrm{cd}}$ and a depth to the neutral axis NA. Thus its moment capacity $M = 0.87A_{\mathrm{s}}f_{\mathrm{y}}z$ can be calculated using the lever arm $z$ for the couple of concrete and rebar steel forces $F_{\mathrm{c}}$ and $F_{\mathrm{t}}$. By specifying the area of steel reinforcement $A_{\mathrm{s}}$ required, e.g. 1–2% of the cross sectional area, and the design bending moment at a cross-section, the required depth $d$ can readily be determined for any given steel yield stress $f_{\mathrm{y}}$.

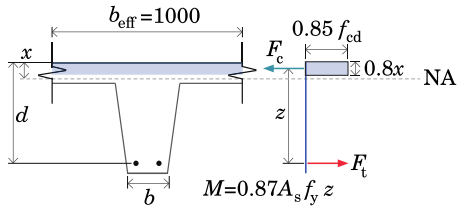


**Fig. 7.** Grillage beam cross-sections can be designed as standard T-beam sections, leveraging a larger effective flange width when under sagging compared to the rectangular beam section width when hogging.

With $r$ as the reinforcement percentage, and given $z = 0.95d$ for sagging and $z = 0.85d$ for hogging, the required depths for sagging $d_{\text{sag}}$ and hogging $d_{\text{hog}}$ can be calculated as follows:

$$d_{\text{sag}} = \sqrt{\frac{100M}{0.87(0.95)rb_{\text{eff}}f_{\text{y}}}} \tag{5}$$

$$d_{\text{hog}} = \sqrt{\frac{100M}{0.87(0.85)rbf_{\text{y}}}} \tag{6}$$

Note that although self-weight is not included in the basic grillage optimization formulation outlined in the previous section, it is straightforward to check that the originally assumed self-weight, applied as a user-defined superimposed dead load, closely matches the self-weight associated with the optimized design, and to if necessary re-run the optimization as part of an iterative process until an acceptable approximation is found. An additional consideration is that at the intersection points between grillage members, some overlap of T-beam volumes will occur, leading to self-weight being somewhat over-estimated; however this effect is likely to be small and for the design problems described herein the volume of intersections were found to be less than 2% of the total volume.

Note that as the grillage optimization procedure uses plastic design concepts, and moment redistribution is implicitly assumed to be possible. This means that, as well as ensuring that each designed cross-section in the structure has the requisite plastic bending capacity, it must also have adequate ductility. This can be achieved by ensuring sections are under-reinforced and that traditional ductile reinforcement bars are used.

## 4. Single bay slab examples

The design of a single 10 m×10 m bay RC floor slab is now considered, with the material efficiency of the proposed optimized grillage system compared with that of both solid flat slab and waffle slab alternatives. A span of 10 m is near the upper-end of what can be economically achieved for a two-way spanning slab, sitting comfortably within the range of what can be achieved using flat slab construction, and near the lower end of what can be achieved using waffle slab construction [53]. Fig. 8 shows the six floor systems compared, where each of the three floor types are considered with both simple edge supports and four fixed corner supports.

For flexural design to Eurocode 2, cross-sections were assessed based on the standard simplified rectangular stress block in compression, while vertical shear was assessed using the strut inclination method. The design code was also used to inform limiting span-to-depths to assess deflections, bar spacing requirements for reinforcement detailing, and for punching shear checks when necessary. An unfactored imposed uniform live loading of 2.5 kPa was taken, using the general office category B1 from Table NA.3 of the UK National Annex [54] to Eurocode 1: Actions on Structures (BS EN 1991-1-1:2002) [55]. An unfactored super-imposed dead loading of 2.35 kPa was applied to all floor slabs as a common allowance for screen,

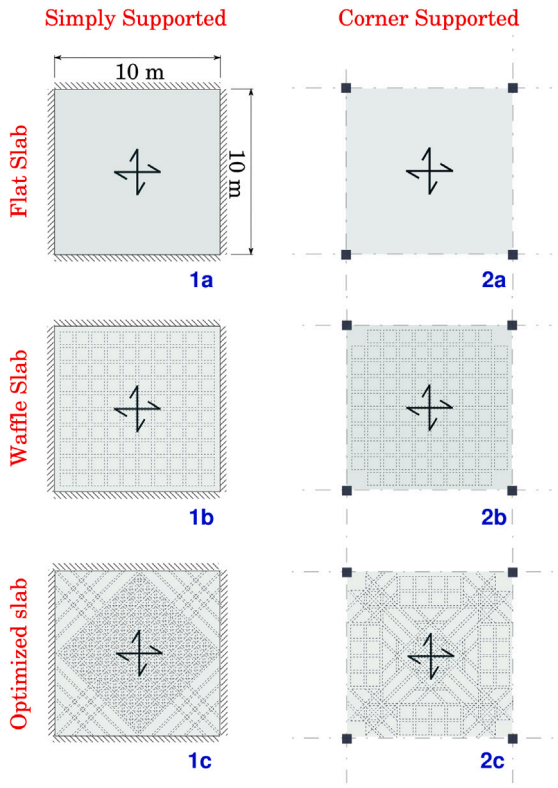


**Fig. 8.** Single bay slab: 1. simply supported on all four sides case, and 2. corner supported on four columns, assumed to provide fixed supports; paired with a. flat slab, b. waffle slab and c. optimized grillage slab.

services and lightweight partitions. Load factors at the structural ultimate limit state for permanent and live actions were taken as $\gamma_{\text{G}} = 1.35$ and $\gamma_{\text{Q}} = 1.5$ respectively from Eurocode 0: Basis of structural design (BS EN 1990:2002+A1:2005) [56] Table A1.2(B), along with appropriate linear combinations for both ultimate and serviceability limit states. Self weight loading using a concrete density of 25 kN/m$^3$ was calculated on a case-by-case basis for each slab design; it was initially estimated for the optimized slabs, as the true self weight is dependant on the final design. A standard concrete strength class of C32/40, a 30 mm concrete cover and Class A high yield steel bars with a characteristic yield strength of 500 N/mm$^2$ was used throughout.

### 4.1. Traditional slab designs

Designs for the flat slabs with differing support conditions were developed. The simply supported flat slab had a depth of 310 mm, while the corner supported flat slab had a depth of 370 mm, these designs are shown in Fig. 9. Excel based spreadsheets are popular among practising engineers and were used in this study to aid all the designs, specifically the RC Spreadsheets version V4D from The Concrete Centre were used. In the first instance a two-way spanning slab design spreadsheet was used, considering detailing requirements for reinforcing bars, hogging and sagging reinforcement requirements, limiting span-to-depth criteria for deflections at the serviceability limit state, as well as details such as additional torsional steel required around the edges (supports). For the flat slab design, and later for the waffle and optimized slab designs, individual bending (also including relevant limiting span-to-depth ratio deflection criteria), shear and punching shear spreadsheets were used, which work in accordance with the relevant sections in BS EN 1990:2002+A1:2005. Moments for the flat slab and waffle slab were calculated using tabular methods, such as can be found in standard design manuals [57], and then apportioned into relevant column and

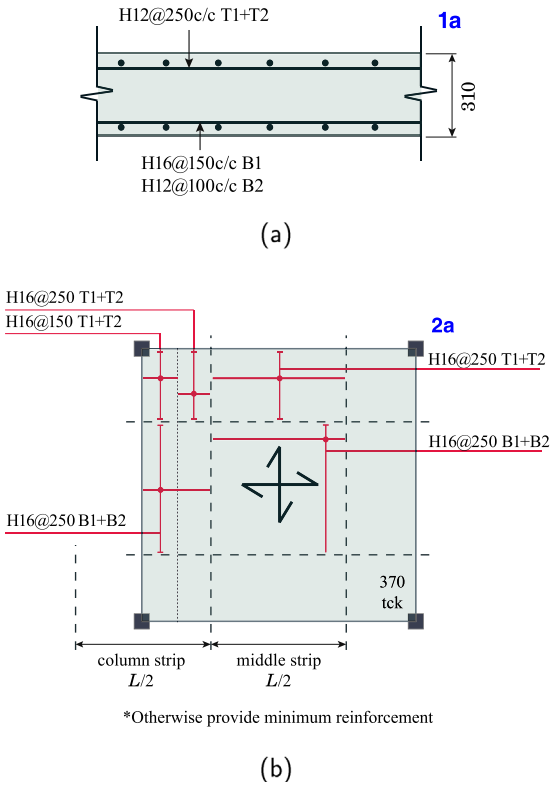


**Fig. 9.** Single bay slab: flat slab design, (a) simply supported case (depth: 310 mm); (b) corner supported case (depth: 370 mm). All dimensions in mm.

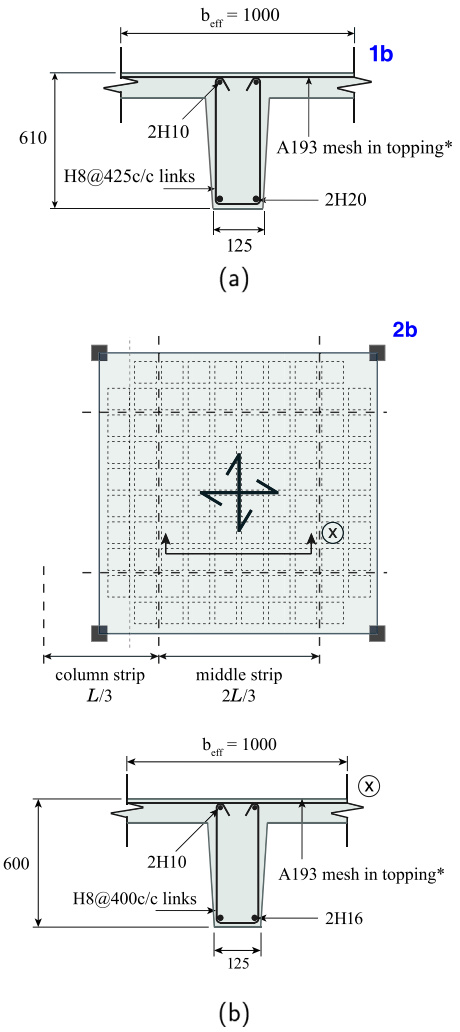


**Fig. 10.** Single bay slab: waffle slab design, (a) simply supported case; (b) corner supported case. All dimensions in mm.

middle strips as per the criteria given in BS EN 1990:2002+A1:2005 Annex I.

For the waffle slabs, constant rib depths were chosen for each of the two support cases, designed to be sufficient to resist the maximum mid-span bending moment and with ribs placed at 1 m centres. In the column supported slab case a solid panel was inserted close to the corner columns to provide adequate punching shear resistance, with necessary shear links designed and detailed. The effective beam width in sagging ($b_{\text{eff}}$ in Eurocode) was taken as the one metre distance between ribs, which is the lower of 20 % the effective beam length and the T-beam spacing. A taper of 4 degrees was used for the downstands of the ribs to facilitate easier striking of the formwork [3]. A 100 mm depth was maintained between ribs largely to meet durability requirements related to concrete cover and an A193 reinforcement mesh was provided for robustness. The same minimum depth and mesh was applied to the optimized slab design. The waffle slab designs are shown in Fig. 10.

### 4.2. Optimized grillage slab designs

Grillage optimization results are shown in Fig. 11; these take account of slab self weight in addition to the specified superimposed dead and live load. Sample extracts from the design of the simply supported slab are shown in Fig. 12; designs for all beam lines in the optimal grillages were developed, taking advantage of symmetry and rationalizing as appropriate. Note that the beams forming the optimized grillages taper along their longitudinal axes, giving linear changes in depth between known cross-section bending moment and shear forces values. A minimum downstand depth was provided at the beam ends, driven by the end shear forces. As with the waffle slabs, a taper angle for the beam cross-section sides of 4 degrees was used for the optimized slabs. For design code deflection checks, each beam in the grillage was conservatively assumed to act as a simply supported beam between its two end points, and verified by limiting their span-to-depth ratio based on BS EN 1990:2002+A1:2005 Clause 7.4.2. With this simplified method, deflections did not govern the design barring one or two instances which resulted in a relatively small (5–10%) increase in rib depth.

### 4.3. Material consumption

The material required for the various single bay slab designs described in the previous sections are presented in Table 1. Considering first the simply supported slab case, it is evident that the optimized grillage requires 42 % less concrete material than the flat slab, whereas the saving in the case of the waffle slab is 18 %. The optimized grillage also requires 31 % less reinforcement than the flat slab, whereas the saving in the case of the waffle slab is 12 %. The observed savings when a waffle slab is employed are similar to those reported previously in [3].

Considering next the column supported slab case, it is seen that the optimized grillage requires 51 % less concrete material than the flat slab, whereas the saving in the case of the waffle slab is lower at 37 %. The optimized grillage also requires 34 % less reinforcement than the flat slab, whereas the saving in the case of the waffle slab is 5 %.

For all considered examples, it has been assumed there are equal hogging and sagging bending moment capacities within the grillage

**Table 1**
Single bay slab: comparison of material consumption requirements for the various slab designs considered (see Fig. 8). All data for an imposed uniform live load of 2.5 kN/m$^2$, super-imposed dead loading of 2.35 kN/m$^2$ and self-weight at 25 kN/m$^3$.

| | 1. Simply supported | | | 2. Corner supported | | |
|---|---|---|---|---|---|---|
| | a. Flat | b. Waffle | c. Optimized | a. Flat | b. Waffle | c. Optimized |
| Concrete weight (kN/m$^2$) | 7.75 | 6.35 | 4.44 | 9.25 | 5.80 | 4.54 |
| Relative self weight | 1 | 0.82 | 0.58 | 1 | 0.63 | 0.49 |
| Reinforcement (kg/m$^2$) | 68.9 | 60.4 | 47.0 | 68.8 | 65.3 | 45.5 |
| Relative reinforcement | 1 | 0.88 | 0.69 | 1 | 0.95 | 0.66 |

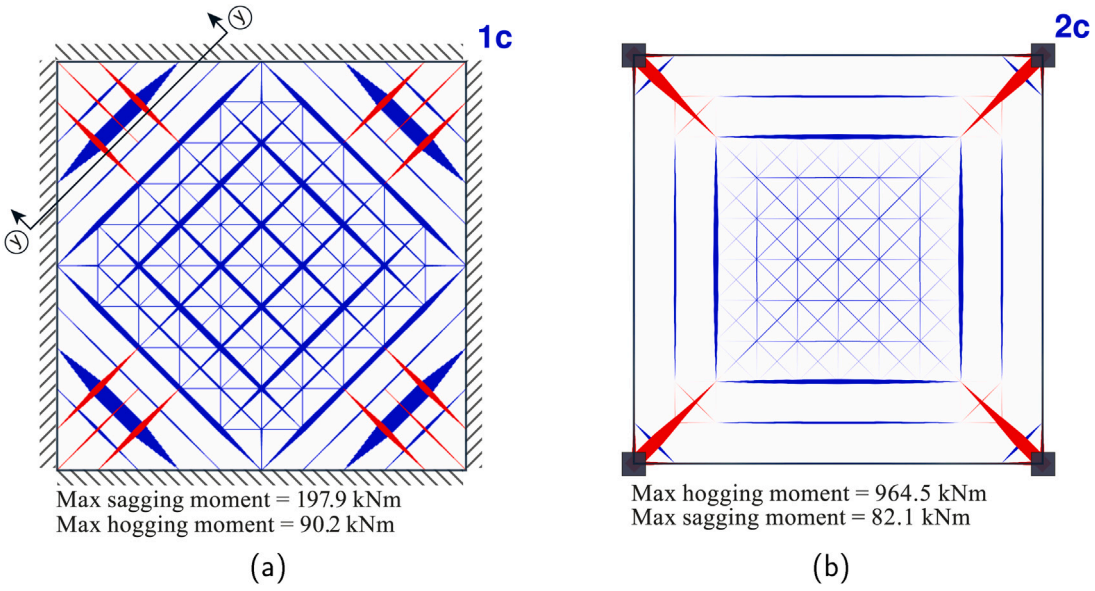


**Fig. 11.** Single bay slab: optimized slab design bending moments, (a) simply supported case; (b) corner supported case. Blue and red lines correspond respectively to sagging and hogging beams, with line-width scaled to the magnitude of the bending moments.

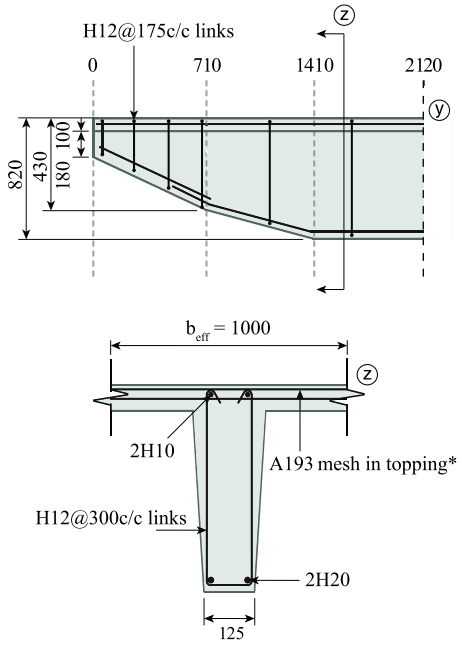


**Fig. 12.** Single bay slab: sample optimized design, showing longitudinal and cross-section of most heavily loaded T-beam in the simply supported slab. All dimensions in mm.

optimization. However, on an individual beam basis or for the entire grillage, different ratios or values of sagging and bending capacity can be used. A study in increasing the proportion of the sagging moment capacity relative to the hogging moment capacity by 25%, was found to lower the volume by a further 10%, while increasing the hogging moment capacity increased the volume.

### 4.4. Influence of varying column positions

Although a building's column layout is always a free parameter in design, architects and engineers have traditionally gravitated towards regularly spaced column grids as a means of rationalizing both the construction process and its internal architecture. This and later sub-sections of this paper, show parametric investigations of moving the locations of columns, to inform the reader to the dramatic improvements on the structural performance and material usage of the resulting floorplates.

The influence of varying the positions of the supporting columns on the optimal grillage volume was explored to see what further material savings could be realized. Thus Fig. 13(a) and (b) respectively show cases where columns were moved inwards from the corners and inwards from the *midpoints* of the slab edges; a full parametric study showing the effects of insetting the columns is also shown in Fig. 14. In all cases a uniform downwards pressure load was applied and both simple and fixed support conditions were considered at the column heads.

From Fig. 14(a) it is evident that the volume of the optimized grillage drops by almost 90 % when the columns are moved inwards from the corners towards the centre of the slab by $0.232L$, the optimal column location for both the simple and fixed column cases. At this

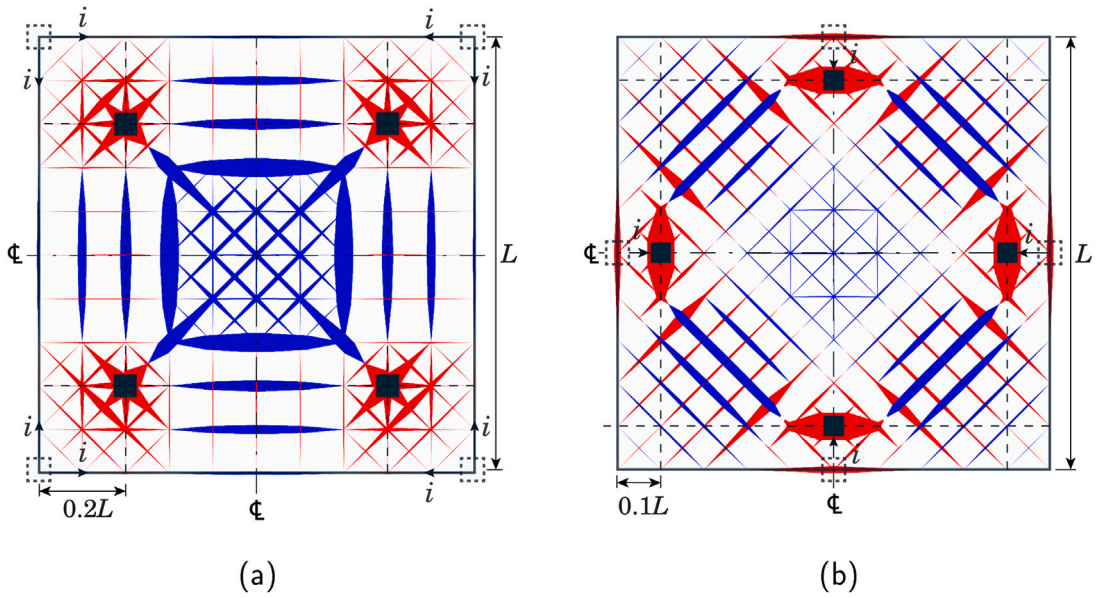


**Fig. 13.** Single bay slab: effects of varying column support positions, with (a) columns inset from corners to near optimal positions at $i = 0.2L$, giving normalized volumes for simply supported and fixed columns of 0.139 and 0.113 (relative to $i = 0$ columns at corners case); (b) columns instead inset from midpoints at $i = 0.1L$, giving normalized volumes for simply supported and fixed columns of 0.163 and 0.150 respectively.

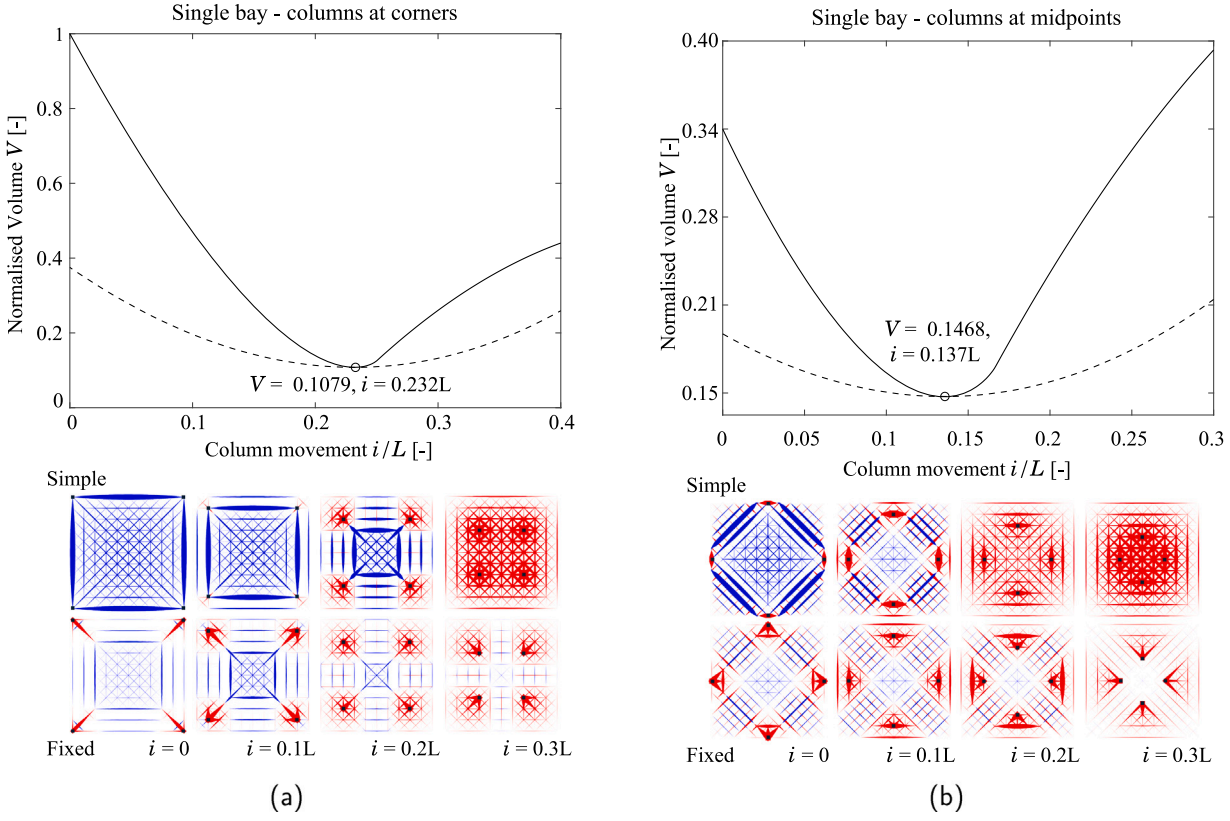


**Fig. 14.** Single bay slab: effects of varying column support positions, showing plots of normalized volume (relative to $i = 0$ columns at corners case) for simply supported columns (solid line) and fixed columns (dashed line) for (a) columns inset from corners case (optimal column location at $i = 0.232L$); (b) columns inset from midpoints case (optimal column location at $i = 0.137L$). 300 data points were used to plot the graphs.

location the spans between columns are reduced, and the presence of hogging moments over the columns has the effect of significantly reducing sagging moments and in turn the overall grillage volume.

Similarly, Fig. 14(b) shows that the grillage volume reduces by 59 % when the midpoint columns are inset by $0.137L$. At the optimal column positions, significant hogging moments over the columns act to reduce the spans of the sagging beams near the centre of the slab. The optimal column locations are again the same for both simple and fixed column cases. These results show that dramatic reductions in the material consumed by a slab can potentially be realized by making changes to the supporting column locations; this finding is also explored further in the next section.

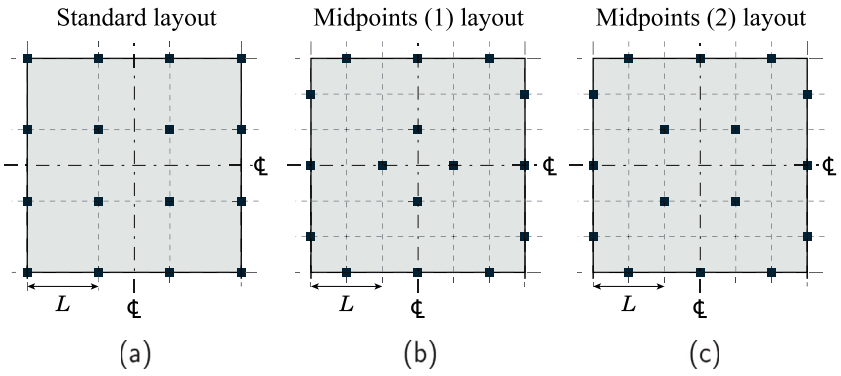


**Fig. 15.** Three-by-three bay floor plate: column layouts investigated, (a) *standard* layout; (b) *midpoints (1)* layout; (c) *midpoints (2)* layout.

## 5. Three-by-three bay floor plate examples

A three-by-three bay floorplate is now considered. Building on the single bay examples considered in the previous section, the effects of varying the positions of columns on the optimum grillage volume were explored. Various column layouts were examined, in all cases assuming a fixed number (16) of supporting columns, as shown in Fig. 15. The first layout considered, denoted *standard*, includes columns positioned at the corners of each bay. Two further layouts were also considered, involving columns located at the mid-sides of each bay, denoted *midpoints (1)* and *midpoints (2)*. Sample optimized grillage solutions are shown in Fig. 16 and a full parametric study showing the effects of insetting the columns for the main scenarios considered is shown in Fig. 17. In all cases a uniform downwards pressure load was applied and both simple and fixed support conditions were considered at the column heads.

In the following multi-bay studies, the imposed vertical loading was applied uniformly across all bays. While different loading arrangements, such as partially loaded bays, could cause specific bays to experience locally higher bending moment magnitudes (and hence lead to larger section sizes), multiple loading scenarios were not a feature of this research. Instead, maximum vertical loading across the floors was used, and is representative of producing the largest total floorplate material volumes so that bulk volume savings could be examined. Due to the linear programming form of the grillage optimization, there would be scope to examine in the future, multiple loadcases for variable distributed loading across bays, as well as other loading scenarios such as including point loads.

Considering first the *standard* layout, the effect of insetting the 12 outer columns from the outer edge of the floor plate is investigated. From Fig. 17(a), it is evident that by moving the outer edge columns inwards by a relatively modest amount, the volume of the optimized grillage is reduced by 50 % and 34 % when simple and fixed supports respectively are involved, occurring respectively when $i = 0.26L$ and $i = 0.30L$. Fig. 16(a) shows this layout with the columns located at $i = 0.3L$, which was the closest location to the minimum volume solution for both fixed and simple support conditions, to an accuracy of $0.1L$. In this case by moving the columns inwards hogging, moments over the column supports have the effect of greatly reducing the sagging moments in the supported beams, thereby reducing the overall structural volume.

Considering next the two *midpoints* layouts, the effect of insetting the 12 outer columns from the outer edge of the floor plate was again investigated. Significant reductions in grillage volume for perimeter column movements of approximately $0.30L$ are evident. For both of the *midpoints* layouts (and also the *standard* layout previously), when columns providing fixed supports were used the calculated optimized grillage volume is lower as they provide greater support to the slab than when simple supports are used. Interestingly, the difference in volume between the simple and fixed case reduces when the columns are near the optimal locations, noting that these were identical for the single bay case considered in Section 4.4. For the *midpoints (1)* case shown in Fig. 16(b), there is significant one-way spanning action between column regions around the perimeter of the floor plate, and although the outer corner columns appear very close together, it is clear this close pairing allows efficient spanning beams between the outer edge and the central bay. The *midpoints (2)* layout was the least efficient when the columns were located on the edge of the floor plate ($i = 0$), with the *standard* layout requiring 25 % less material, and the *midpoints (1)* layout requiring 39 % less material for the simple supports case.

Overall, when the columns were inset by the distances leading to their respective lowest volumes, the *standard* layout was found to be most efficient, requiring 11 % less material than *midpoints (2)* and 16 % less material than *midpoints (1)* for the simple supports case. This is consistent with what was observed in supplementary single bay studies, where it was found that when columns were placed at the midpoints of the edges of the slab there was little benefit in insetting these, whereas the corner column layout was most efficient when the columns were inset. A visualization of the *midpoints (1)* layout is shown in Fig. 18.

It is also of interest to investigate the effect of moving the four internal columns outwards from the centre of the floor plate, with the outer columns remaining located at the perimeter. This showed less impressive volume reductions than when the outer columns were inset. For example with the simply-supported cases, the *standard* layout grillage volume reduction was 8 % while for the *midpoints (1)* layout a more significant 24 % reduction was obtained (see Fig. 16(d)), and for *midpoints (2)* the volume reduction was just 7 % (relative to i = 0 for each case respectively, the corresponding values relative to $i = 0$ columns in the standard layout case are 8 %, 5 % and 17 %). When fixed support conditions were implemented at the columns, the volume reductions were even less than for the simply supported cases. This indicates that most reduction in material volume can be realized by insetting the outer columns from the perimeter, which has the effect of "lifting" the bending moment diagram by generating hogging bending moments over the columns.

Finally, note that for simplicity in the studies a single load case has been assumed, but, particularly due to the presence of cantilever sections, multiple pattern load case scenarios should also be considered to confirm the range of applicability of the findings. Also, here the column positions have been adjusted manually, but it would be of interest to use optimization to seek the optimal positions of columns supporting a floor plate, as has been done e.g. in [58] for elastic plate problems.

## 6. Discussion

The single and multi-bay floor studies described in the previous sections provoke discussion in the following areas: (1) fabrication, (2) digital workflow, (3) engineering, and (4) architecture.

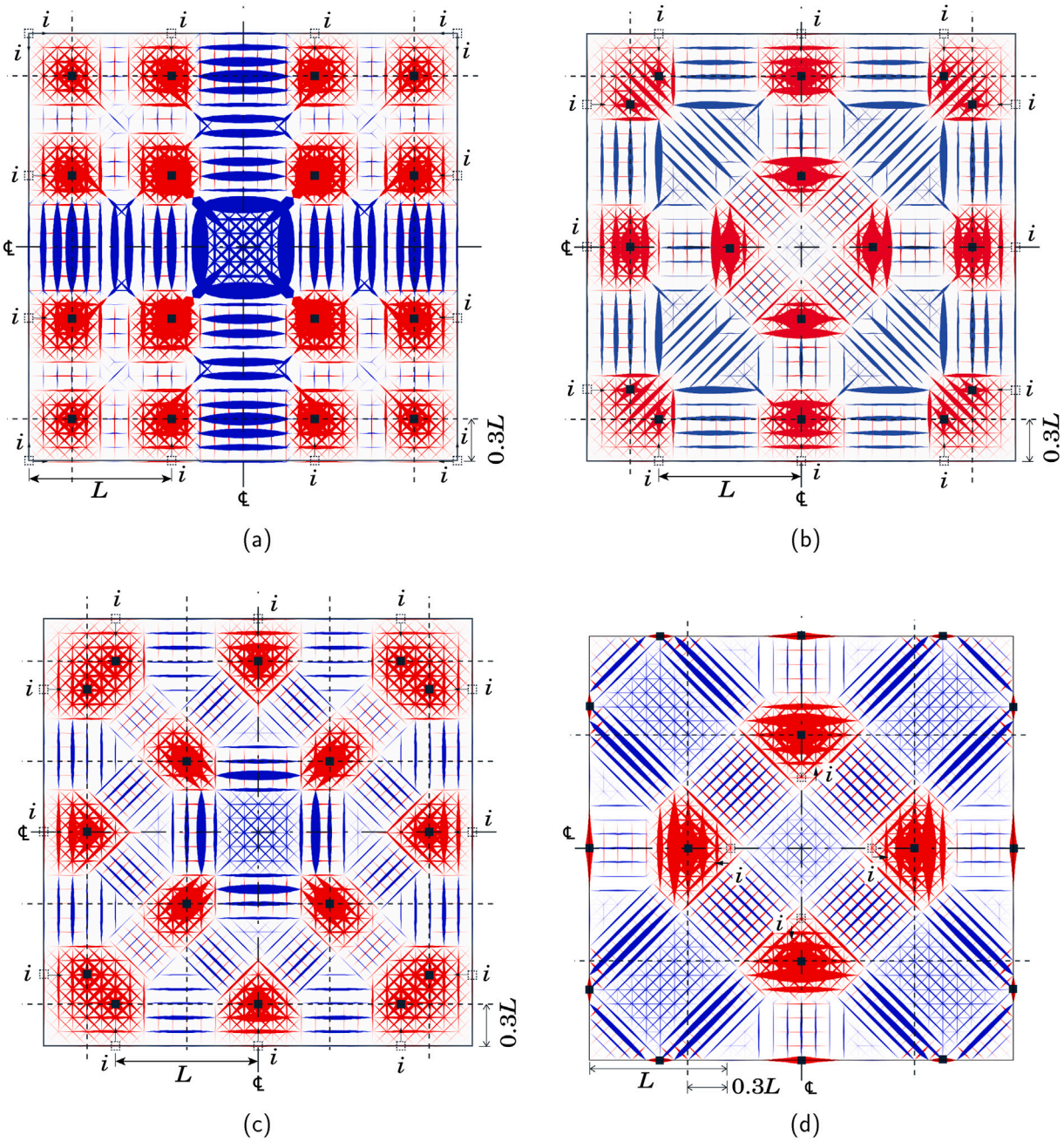


**Fig. 16.** Three-by-three bay floor plate, optimized grillage layouts for simple column supports: (a) for *standard* floor plate with outer columns inset to $i = 0.3L$ giving normalized volume of $V = 0.5181$ (relative to $i = 0$ columns in the standard layout case); (b) for *midpoints (1)* floor plate with outer columns inset to $i = 0.3L$ giving normalized volume of $V = 0.5900$; (c) for *midpoints (2)* floor plate with outer columns inset to $i = 0.3L$ giving normalized volume of $V = 0.5500$; (d) for the *midpoints (1)* floor plate with inner columns moved outwards to a near optimal position of $i = 0.3L$ giving normalized volume of $V = 0.9525$.

### 6.1. Fabrication

Despite the significant material weight savings that can be achieved from designing floor slabs as structural grillages, the additional fabrication complexity clearly has the potential to inhibit uptake in practice. Currently the costs of the concrete and steel materials used in construction are relatively low compared to the cost of the complex formwork needed to construct the optimized grillage geometries identified herein, negating the financial incentive to design with less material. However, there is growing pressure for more sustainable building designs, with the structural engineer potentially having a key role to play in reducing embodied carbon. Additionally, as pointed out in the introduction, new types of digital fabrication for concrete formworks are being prototyped and brought to market, that could potentially be employed for the optimal grillage geometries, making use of floor plate symmetry, standard design cases, and creating formwork suitable for repeated use. Given that the proposed elements have a flat topside, only a single sided formwork would be needed (similar to waffle slabs), meaning that if a formwork is made that is reusable, it can be easily used/struck multiple times for creating repeating elements. While a benefit of the presented optimized grillage system is the use of standard steel reinforcement bars, fabrication complexity is increased by the presence of tapering beams that require a wide range of rebar bend angles, lapping and anchorage details, and variable depth shear links. Other points of note include the need to include chamfers in the designed cross-sections to facilitate de-moulding, and the choice of concrete mix design to ensure adequate compaction of the concrete can be achieved.

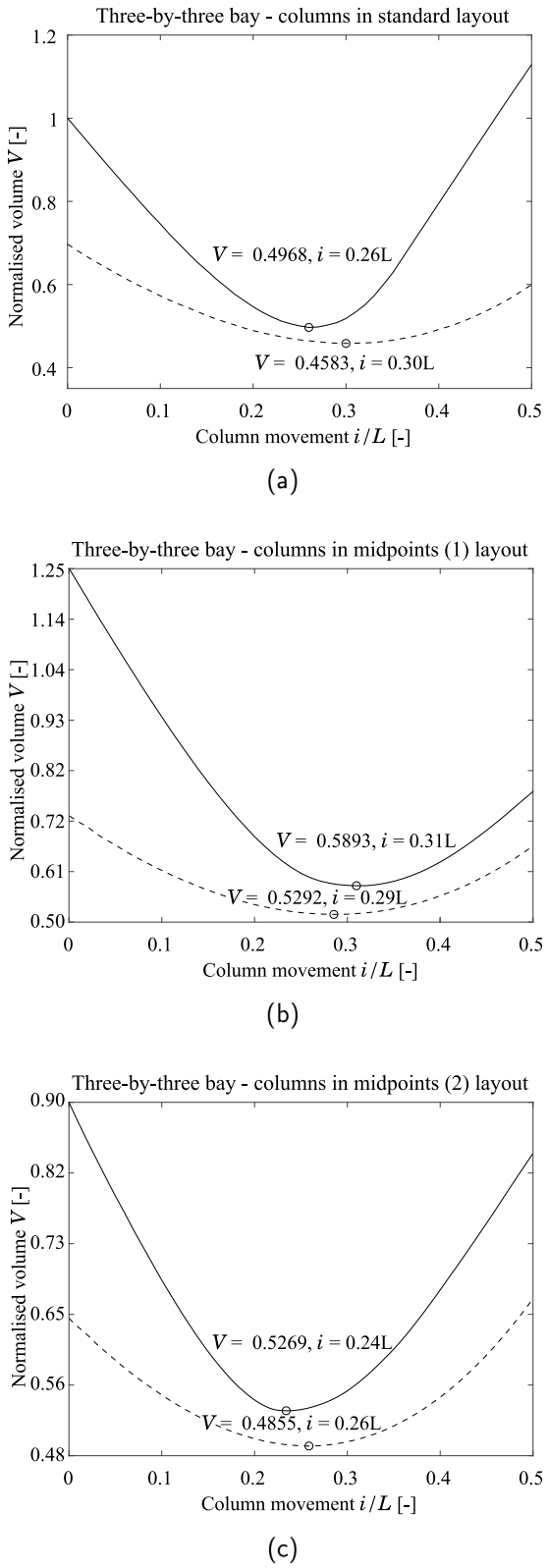


**Fig. 17.** Three-by-three bar floor plate: effects of varying column support positions, showing plots of normalized volume (relative to $i = 0$ columns in the standard layout case) for simply supported columns (solid line) and fixed columns (dashed line) for, (a) *standard* floor plate; (b) *midpoints (1)* floor plate; (c) *midpoints (2)* floor plate. 50 data points were used to plot the graphs.

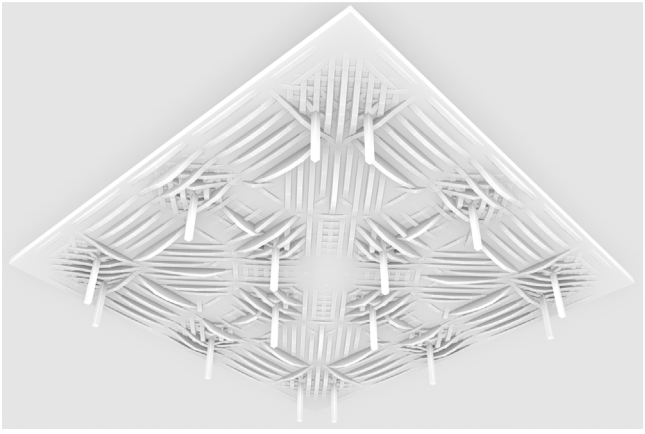

**Fig. 18.** Three-by-three bar floor plate: visualization of the optimized grillage geometry for the simply supported columns case in the *midpoints (1)* layout. Columns are shown near their optimal locations, at $i = 0.3L$.

### 6.2. Digital workflow

A benefit of the presented workflow is that relatively little post-processing of the output from the grillage optimization is required. Using only adjacent member connectivity in the optimization leads to a clean grillage topology, for which section depths are easily derived. The linear programming solver that is used to obtain optimized grillage solutions can produce designs in a matter of seconds on a desktop computer, facilitating the rapid exploration of different floor plate geometries and the placement of columns at the early conceptual design stage of a project. Although a feedback loop was performed in which the calculated grillage volumes were used to update the initial assumed self-weight dead-loads with a number of iterations required for convergence, it would be possible to instead include self-weight in the optimization process directly. The engineering calculations to design code standards were performed manually and with design aids such as spreadsheets, but it would be straightforward to perform these calculations automatically, enabling sizing and detailing reinforcement to be generated directly from the bending moments and shear forces associated with the grillage optimization solution. This final engineering design could then be passed to a digital fabrication process, with a CNC system used to shape the formwork, and with limited manual intervention and labour.

### 6.3. Engineering

As discussed in Section 2, the beams in the grillage were individually assessed for deflection in isolation, assuming that they were simply supported between two points of contra-flexure. In reality, deflections will be influenced by the connectivity of the beams at the joints. As such, deflections could be computed more accurately, with design code deflection constraints imposed as part of the workflow. The torsional resistance of the beams is neglected in the grillage optimization formulation described, which assumes that externally applied loads are resisted entirely by bending moments in the beams forming the grillage structure. In reality, some of the applied load may be taken by the torsional resistance of the T-beam cross-sections, which has torsional capacity from the downstands and shear links, as well as from the concrete slab topping.

### 6.4. Architecture

Beyond the engineering design of the grillage floors, this study has the potential to provoke a complete rethinking of how floor plates are configured. In particular, the locations of supporting columns have

been shown to have a significant first order effect on the overall volume of material required to form the floor plate. This has the potential to stimulate architects to rethink where the facade line should be in our buildings, the effect on mullions, and promoting the greater use of cantilevering and external balconies. As well as greatly reducing the volume of material consumed, switching from traditional orthogonal column grids to more bespoke column layouts that are influenced by the structural force flow, also gives rise to different sight-lines and corridor/circulation routes. Some of the presented optimized grillage layouts show central "hub" areas forming in the floor plate, or hint at the potential for satellite "breakout" areas. Exposing the soffit of the grillage system, with its undulating and radiating ribs, would also give building occupants a greater appreciation of the structural system employed. Finally, the locations of exposed ribs will affect the solutions for services integration and the acoustic properties of the building.

## 7. Conclusions

A new reinforced concrete grillage floor system has been presented, which uses a grillage layout optimization formulation to inform the engineering design of T-beam cross-sections. Unlike a traditional waffle slab of fixed overall depth, the optimized grillage floor utilizes variable depth tapered ribs to carry bending moments, leading to significant savings in the quantities of both concrete and steel reinforcement material.

For a single bay of a building, detailed design code compliant solutions were developed for flat slabs, waffle slabs and optimized grillage slabs. This study demonstrated the significant sustainability advantage of the optimized grillage floor system, as it was found to save 42–51 % in concrete material compared to the flat slab, and 18–37 % compared to the waffle slab. Reinforcement demand was also reduced by 31–34 % compared to the flat slab, whereas the savings in the case of the waffle slab were 5–12 %.

The research further demonstrated material saving advantages, by pairing the grillage optimization workflow with repositioned supporting columns, or use of a different column grid layout. For the three-by-three bay floor plate studies, encouraging additional cantilevering action by insetting perimeter columns was found to reduce the optimal grillage volume by over 50 % for a standard grid layout. Various non-standard column layouts were also investigated, which showed that similar material savings of 40–58 % could be achieved by insetting perimeter columns. This is due to "lifting up" the bending moment diagrams by inducing hogging moments over the columns, and forming additional internal support lines for more efficient load take-down.

Although buildability questions remain, the optimized grillage floor system has the potential to greatly reduce the embodied carbon footprint associated with structures such as multi-storey buildings, that make frequent use of flat slabs and regular column grids. Reduced superstructure material requirements in turn also leads to reduced loads on substructure elements such as piled or raft foundations, reducing the volume of material required for the whole building.

## Declaration of competing interest

The authors declare that they have no known competing financial interests or personal relationships that could have appeared to influence the work reported in this paper.

## References


[1] Feld Jacob, Carper Kenneth L. Construction failure. 1st ed.. John Wiley & Sons; 1996.

[2] Concrete framed buildings: A guide to design and construction. 1st ed.. MPA The Concrete Centre; 2006.

[3] Burridge Jenny, Toogood Elaine. Return of the rib. Concr Q 2019;(268):16–8.

[4] Hawkins Will, Orr John, Shepherd Paul, Ibell Tim. Design, construction and testing of a low carbon thin-shell concrete flooring system. In: Structures, Vol. 18. Elsevier; 2019, p. 60–71.

[5] Lai Tina. Structural behavior of BubbleDeck® slabs and their application to lightweight bridge decks (Master's thesis), Massachusetts Institute of Technology, Dept. of Civil and Environmental Engineering; 2010.

[6] Investigation results - Eindhoven airport parking garage. 2017, URL https://www.bam.com/en/press/press-releases/2017/9/investigation-results-known-of-technical-cause-partial-collapse.

[7] Hertz Kristian Dahl, Castberg Niels Andreas, Christensen Jacob. Super-light concrete decks for building floor slabs. Struct Concr 2014;15(4):522–9.

[8] Halpern Allison B, Billington David P, Adriaenssens Sigrid. The ribbed floor slab systems of pier luigi nervi. In: Proceedings of the international association for shell and spatial structures, Vol. 2013. International Association for Shell and Spatial Structures (IASS); 2013, p. 1–7.

[9] Nervi Pier Luigi. Aesthetics and technology in building: The twenty-first-century edition. University of Illinois Press; 2018.

[10] Masson-Delmotte V, Zhai P, Pörtner H-O, Roberts D, Skea J, Shukla PR, Pirani A, Moufouma-Okia W, Péan C, Pidcock R, Connors S, Matthews JBR, Chen Y, Zhou X, Gomis MI, Lonnoy E, Maycock T, Tignor M, Waterfield T, editors. Global Warming of 1.5ºC. An IPCC Special Report on the impacts of global warming of 1.5ºC above pre-industrial levels and related global greenhouse gas emission pathways, in the context of strengthening the global response to the threat of climate change, sustainable development, and efforts to eradicate poverty. 2018.

[11] Pérez-Lombard Luis, Ortiz José, Pout Christine. A review on buildings energy consumption information. Energy Build 2008;40(3):394–8.

[12] Abergel Thibaut, Dean Brian, Dulac John. Towards a zero-emission, efficient, and resilient buildings and construction sector: Global status report 2017, Vol. 22. UN Environment and International Energy Agency; 2017.

[13] Ibn-Mohammed Taofeeq, Greenough Rick, Taylor S, Ozawa-Meida Leticia, Acquaye Adolf. Operational vs embodied emissions in buildings — A review of current trends. Energy Build 2013;66:232–45.

[14] Davis Steven J, Lewis Nathan S, Shaner Matthew, Aggarwal Sonia, Arent Doug, Azevedo Inês L, Benson Sally M, Bradley Thomas, Brouwer Jack, Chiang Yet-Ming, et al. Net-zero emissions energy systems. Science 2018;360(6396).

[15] Humphreys Ken, Mahasenan M. Towards a sustainable cement industry - Substudy 8: Climate change. World Business Council for Sustainable Development; 2002.

[16] Andrew Robbie M. Global CO2 emissions from cement production. Earth Syst Sci Data 2018;10(1):195–217.

[17] Kelly Thomas D, Matos Grecia R, Buckingham David A, DiFrancesco Carl A, Porter Kenneth E. Historical statistics for mineral and material commodities in the United States. In: US geological survey data series, Vol. 140. 2010, p. 01–06.

[18] Boden TA, Marland G, Andres RJ. Global, regional, and national fossil-fuel CO2 emissions, Vol. 1. Oak Ridge, Tenn., USA: Carbon Dioxide Information Analysis Center, Oak Ridge National Laboratory, US Department of Energy; 2017.

[19] Meyer Christian. The greening of the concrete industry. Cem Concr Compos 2009;31(8):601–5.

[20] Allwood Julian M, Ashby Michael F, Gutowski Timothy G, Worrell Ernst. Material efficiency: A white paper. Resour Conserv Recy 2011;55(3):362–81.

[21] Crow James Mitchell. The concrete conundrum. Chem World 2008;5(3):62–6.

[22] De Wolf Catherine, Ramage Michael, Ochsendorf John. Low carbon vaulted masonry structures. J Int Assoc Shell Spat Struct 2016;57(4):275–84.

[23] Foraboschi Paolo, Mercanzin Mattia, Trabucco Dario. Sustainable structural design of tall buildings based on embodied energy. Energy Build 2014;68:254–69.

[24] Liew Andrew, López D López, Van Mele Tom, Block Philippe. Design, fabrication and testing of a prototype, thin-vaulted, unreinforced concrete floor. Eng Struct 2017;137:323–35.

[25] May Sebastian, Michler Harald, Schladitz Frank, Curbach Manfred. Lightweight ceiling system made of carbon reinforced concrete. Struct Concr 2018;19(6):1862–72.

[26] Kromoser Benjamin, Preinstorfer Philipp, Kollegger Johann. Building lightweight structures with carbon-fiber-reinforced polymer-reinforced ultra-high-performance concrete: Research approach, construction materials, and conceptual design of three building components. Struct Concr 2019;20(2):730–44.

[27] Ghavami Khosrow. Bamboo as reinforcement in structural concrete elements. Cem Concr Compos 2005;27(6):637–49.

[28] Pilakoutas Kypros, Neocleous Kyriacos, Tlemat Houssam. Reuse of tyre steel fibres as concrete reinforcement. Proc ICE - Eng Sustain 2004;157(3):131–8.

[29] Veenendaal Diederik, West Mark, Block Philippe. History and overview of fabric formwork: using fabrics for concrete casting. Struct Concr 2011;12(3):164–77.

[30] Yang Yuanzhang, Orr John, Ibell Tim. Shear behaviour of fabric formed t beams reinforced using W-FRP. In: Structures, Vol. 24. Elsevier; 2020, p. 869–79.

[31] Jewett Jackson L, Carstensen Josephine V. Topology-optimized design, construction and experimental evaluation of concrete beams. Autom Constr 2019;102:59–67.

[32] Jewett Jackson L, Carstensen Josephine V. Experimental investigation of strut and tie layouts in deep RC beams designed with hybrid bi-linear topology optimization. Eng Struct 2019;197:109322.

[33] Lavery Conor. Spencer dock bridge. Concr Int 2013;35(6):28–31.

[34] Li Lin, Yan Jihong, Xing Zhongwen. Energy requirements evaluation of milling machines based on thermal equilibrium and empirical modelling. J Clean Prod 2013;52:113–21.

[35] Søndergaard Asbjørn, Feringa Jelle, Stan Florin, Maier Dana. Robotic abrasive wire cutting of polymerized styrene formwork systems for cost-effective realization of topology-optimized concrete structures. Constr Robot 2018;2(1–4):81–92.
[36] Grünewald Steffen, Schipper Roel. Transition from fluid to solid concrete in the flexible mould process. In: RILEM international conference on concrete and digital fabrication. Springer; 2020, p. 262–71.
[37] Meibodi Mania Aghaei, Jipa Andrei, Giesecke Rena, Shammas Demetris, Bernhard Mathias, Leschok Matthias, Graser Konrad, Dillenburger Benjamin. Smart slab: Computational design and digital fabrication of a lightweight concrete slab. In: Acadia 2018 recalibration: On imprecision and infidelity: proceedings of the 38th annual conference of the association for computer aided design in architecture. Association for Computer Aided Design in Architecture (ACADIA); 2018, p. 434–43.
[38] Rippmann Matthias, Liew Andrew, Van Mele Tom, Block Philippe. Design, fabrication and testing of discrete 3D sand-printed floor prototypes. Mater Today Commun 2018;15:254–9.
[39] Hansemann Georg, Schmid Robert, Holzinger Christoph, Tapley Joshua, Kim Hoang Huy, Sliskovic Valentino, Freytag Bernhard, Trummer Andreas, Peters Stefan. Additive fabrication of concrete elements by robots: Lightweight concrete ceiling. In: Fabricate 2020: Making resilient architecture. UCL PRESS; 2020, p. 124–9.
[40] Buswell Richard A, da Silva WR Leal, Bos Freek P, Schipper HR, Lowke Dirk, Hack Norman, Kloft Harald, Mechtcherine Viktor, Wangler Timothy, Roussel Nicolas. A process classification framework for defining and describing digital fabrication with concrete. Cem Concr Res 2020;134:106068.
[41] Wangler Timothy, Lloret Ena, Reiter Lex, Hack Norman, Gramazio Fabio, Kohler Matthias, Bernhard Mathias, Dillenburger Benjamin, Buchli Jonas, Roussel Nicolas, et al. Digital concrete: opportunities and challenges. RILEM Tech Lett 2016;1:67–75.
[42] Asprone Domenico, Menna Costantino, Bos Freek P, Salet Theo AM, Mata-Falcón Jaime, Kaufmann Walter. Rethinking reinforcement for digital fabrication with concrete. Cem Concr Res 2018;112:111–21.
[43] Bolbotowski Karol, He Linwei, Gilbert Matthew. Design of optimum grillages using layout optimization. Struct Multidiscip Optim 2018;58(3):851–68.
[44] Dorn W, Gomory RE, Greenberg H. Automatic design of optimal structures. J Mec 1964;3:25–52.
[45] Gilbert Matthew, Tyas Andrew. Layout optimization of large-scale pin-jointed frames. Eng Comput 2003;20(8):1044–64.
[46] Rozvany GIN. Optimal design of flexural systems: Beams, grillages, slabs, plates and shells. Pergamon; 1976.
[47] Muspratt MA. Destructive tests on rationally designed slabs. Mag Concr Res 1970;22(70):25–36.
[48] Stoiber Nadine, Kromoser Benjamin. Topology optimization in concrete construction: a systematic review on numerical and experimental investigations. Struct Multidiscip Optim 2021;64:1725–49.
[49] Buswell Richard A, Soar Rupert C, Gibb Alistair GF, Thorpe A. Freeform construction: mega-scale rapid manufacturing for construction. Autom Constr 2007;16(2):224–31.
[50] Tena-Colunga Arturo, Chinchilla-Portillo Karen Lineth, Juárez-Luna Gelacio. Assessment of the diaphragm condition for floor systems used in urban buildings. Eng Struct 2015;93:70–84.
[51] British Standards Institution. Eurocode 2: Design of concrete structures - Part 1-1: General rules and rules for buildings. British Standards Institution; 2004.
[52] British Standards Institution. UK national annex to eurocode 2: Design of concrete structures - Part 1-1: General rules and rules for buildings. British Standards Institution; 2004.
[53] Goodchild CH, Webster RM, Elliott KS. Economic concrete frame elements to Eurocode 2. MPA The Concrete Centre; 2009.
[54] British Standards Institution. UK national annex to eurocode 1: Actions on structures - Part 1-1: General — Densities, self-weight, imposed loads for buildings. British Standards Institution; 2002.
[55] British Standards Institution. Eurocode 1: Actions on structures - Part 1-1: General — Densities, self-weight, imposed loads for buildings. British Standards Institution; 2002.
[56] British Standards Institution. Eurocode 1: Eurocode — Basis of structural design. British Standards Institution; 2002.
[57] Bond AJ, Brooker O, Harris AJ, Harrison T, Moss RM, Narayanan RS, Webster R. How to design concrete structures using Eurocode 2. MPA The Concrete Centre; 2006.
[58] Jang Gang-Won, Shim Ho Seong, Kim Yoon Young. Optimization of support locations of beam and plate structures under self-weight by using a sprung structure model. J Mech Des 2009;131(2).